FEBS Letters 560 (2004) 134–140 FEBS 28102

Correlation between conformation and antibody binding: NMR structure of cross-reactive peptides from *T. cruzi*, human and *L. braziliensis*

M.R. Soares[a,b], P.M. Bisch[a], A.C. Campos de Carvalho[a,c], A.P. Valente[b], F.C.L. Almeida[b,*]

[a] *Instituto de Biofísica Carlos Chagas Filho, Universidade Federal do Rio de Janeiro, 21941-590 Rio de Janeiro, RJ, Brazil*
[b] *Centro Nacional de Ressonância Magnética Nuclear, Departamento de Bioquímica Médica – ICB/CCS, Universidade Federal do Rio de Janeiro, Av. Brigadeiro Trompowiski s/n, CCS, Bloco E sala 10, 21941-590 Rio de Janeiro, RJ, Brazil*
[c] *Albert Einstein College of Medicine, Bronx, NY 10461, USA*

Received 1 December 2003; revised 8 January 2004; accepted 12 January 2004

First published online 4 February 2004

Edited by Thomas L. James

Abstract The structure of peptides corresponding to the C-terminal residues from *Trypanosoma cruzi* (R13), human (H13) and *Leishmania braziliensis* (A13) ribosomal proteins were determined using nuclear magnetic resonance. Although there is only one amino acid difference between them, the peptides present distinct structures in solution: R13 adopts a random coil conformation while H13 and A13 form a bend. Interaction of these peptides with polyclonal antibodies from chronic Chagas' disease patients and a monoclonal antibody raised against *T. cruzi* ribosomal P2β protein was probed by transferred NOE. The results show that the flexibility of R13 is fundamental for the binding to the antibody.

Key words: Ribosomal P protein; Chagas' disease; Nuclear magnetic resonance; Molecular recognition

1. Introduction

Chronic Chagas' heart disease (cChHD) is the most frequent and severe clinical consequence of infection with *Trypanosoma cruzi* [1]. The mechanisms responsible for the cardiomyopathy are not clearly understood, but the occurrence of chronic myocardial injury in the near absence of parasites suggests an autoimmune mechanism [2]. Nevertheless, the hypothesis of an autoimmune disorder in Chagas' disease remains controversial. Thus, cardiomyopathy might result from a parasite-induced activation of the immune system leading to a breakdown of tolerance for self-antigens [3]. Another possibility involves a *T. cruzi*-induced cross-reactive immune response to self-antigens through a molecular mimicry-dependent mechanism [4]. Indeed, immune responses developed against self-antigens via molecular mimicry-dependent mechanisms have been shown to play a role in autoimmune phenomena associated with infectious disease [4–6]. Several *T. cruzi* antigens have been reported to present epitopes similar to mammalian antigens, including the family of trypomastigote-specific FI-160 antigens [7,8], the microtubule-associated protein [9], the cardiac myosin antigen (B13) [10], and members of the ribosomal P protein family [11–13].

Patients with cChHD present a high titer of antibodies against the C-terminal end of the ribosomal P protein of *T. cruzi*, which has high similarity to the C-terminal region of human ribosomal P proteins and also to the second loop of the human β-adrenergic [13] and M2 muscarinic receptors [14]. As the sera of these patients can elicit heart function disturbances, several researchers believe that the primary sequence similarity is related to the observed cross-reactivity of antibodies from cChHD patients with the heart receptors [14].

In rabbit heart preparations, electrical disturbances can be alleviated if the patients' sera are incubated with small peptides corresponding the C-terminal region of the P ribosomal proteins from humans and *T. cruzi*, but not from *Leishmania braziliensis* [14]. Primary sequence comparison (Table 1) shows that the three peptides differ in only one amino acid, therefore the A13 result is not compatible with a linear charged epitope (EEXDDD, R13 = E; H13 = S; A13 = A).

In an effort to understand the structural basis for the cross-reactivity, we determined the structure of R13, H13 and A13 peptides by nuclear magnetic resonance (NMR) spectroscopy. Transferred nuclear Overhauser effect spectroscopy (NOESY) experiments were used to probe interaction and conformational changes upon antibody binding. The results showed different degrees of flexibility for each peptide and this effect may result in different degrees of recognition by antibodies. In that regard, the tendency of A13 to form a more stable structure in solution can impair antibody recognition and explain the lack of inhibition of cChHD patients' sera by the *L. braziliensis*-derived peptide.

2. Materials and methods

2.1. Sample preparation

Sequences of the peptides used for the present study are shown in Table 1. The first sequence corresponds to the C-terminus of the

Table 1
Sequence of peptides derived of ribosomal P protein

Name	Sequence number	Sequence	Origin
R13	107–119	EEEDDDMGFGLFD	*T. cruzi*
H13	102–115	EESDDDMGFGLFD	Human
A13	93–105	EEADDDMGFGLFD	*L. braziliensis*

*Corresponding author. Fax: (55)-21-25626756.
E-mail address: falmeida@cnrmn.bioqmed.ufrj.br (F.C.L. Almeida).

0014-5793/04/$30.00 © 2004 Published by Elsevier B.V. on behalf of the Federation of European Biochemical Societies.
doi:10.1016/S0014-5793(04)00088-2

T. cruzi P ribosomal protein. H13 is a peptide derived from the human P ribosomal protein. A13 is derived from the *L. braziliensis* P ribosomal protein. All peptides were synthesized by Research Genetics, purified by high performance liquid chromatography, and checked by mass spectroscopy.

2.2. Production of the antibodies

The monoclonal antibody (mAb) used was kindly provided by M.J. Levin. The mAb production and characterization are described in [15].

We used polyclonal antibodies (pAb), obtained from a group of cChHD patients, that were previously functionally characterized [14]. Purification of the IgG fraction was performed by serum precipitation with ammonium sulfate (40%), followed by overnight dialysis against phosphate buffer (pH 8.0) and chromatography in a DEAE matrix under continuous addition of phosphate buffer (pH 8.0).

2.3. Preparation of NMR samples

For NMR experiments the samples were prepared in 10% D_2O (99.9%, Isotec) using 10 mM phosphate buffer at pH 5.5. The peptide concentration was 2 mM for free peptide experiments. The peptide:pAb molar ratio was 20:1 and the peptide:mAb molar ratio was 100:1 for transfer NOE experiments.

2.4. NMR spectroscopy

The NMR experiments for the free peptides were performed at 5°C and 20°C and experiments for peptides in the presence of antibodies were conducted at 20°C. NMR spectra were obtained in a Bruker Avance DRX600 spectrometer operating at 600.04 MHz. Water suppression was achieved using the WATERGATE technique [16]. Total correlation spectroscopy (TOCSY) spectra (spin-lock time of 70 ms) were acquired using the MLEV-17 pulse sequence [17]. NOESY [18] and transfer NOESY [19] spectra were acquired using a 150 ms mixing time. The spectra were processed using NMRPIPE [20].

In order to establish the fast change between free and bound states to transfer NOESY experiments we tested different pH values and temperatures. This condition occurs in the pH range of 5.5–6.5 and 20°C. The transfer NOESY experiments required more time acquisition (about 24 h) due to lower peptide and antibody concentrations.

2.5. NOE data analysis and structure calculation

All NMR spectra were analyzed using NMRVIEW, version 5.0.3 [21]. NOE cross-peaks were integrated in the NOESY spectra and their intensities were converted to distances, which were calibrated using the equations suggested by Hybert et al. [22]. The structure calculations were performed using CNS_Solve version 1.1 [23]. Starting with the extended structure, 100 structures were generated using the torsion angle simulated annealing protocol [24]. This was followed by 10 000 steps of simulated annealing at 5000 K and a subsequent decrease in the temperature in 20 000 steps in the first slow-cool annealing stage. All the structures were analyzed with the program MOLMOL [25].

3. Results

3.1. Chemical shift and restraint assignments

The chemical shift assignments of the peptides were per-

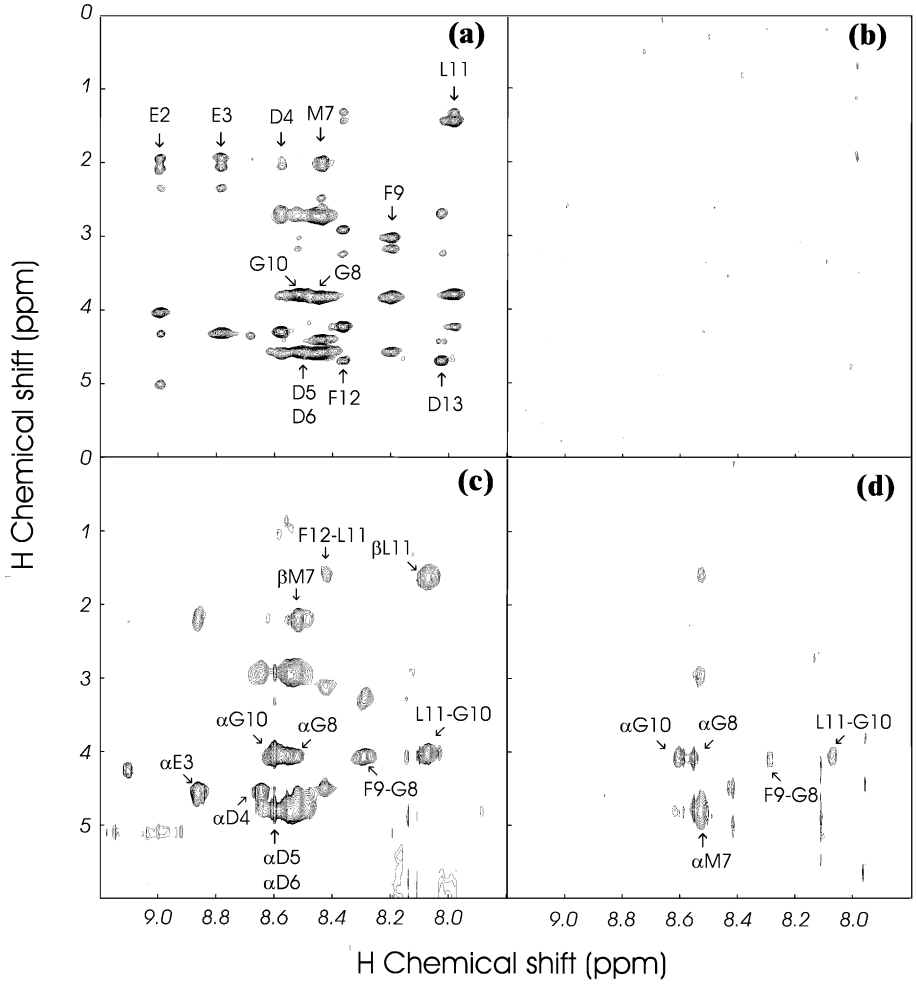

Fig. 1. Amide region of ^{1}H NMR spectra of R13 in phosphate buffer. a: NOESY spectrum at 5°C of 2 mM R13, 80 scans. b: NOESY spectrum at 20°C of 2 mM R13, 80 scans. c: Transfer NOESY spectrum of the mixture of 1 mM R13 and 50 μM pAb at 20°C, 384 scans. d: Transfer NOESY spectrum of the mixture of 1 mM R13 and 10 μM mAb at 20°C, 384 scans.

formed through TOCSY and NOESY spectra obtained at 5°C (Figs. 1a, 2a and 3a) by the sequential strategy as proposed by Wüthrich [26]. Sequential connectivities could be observed through $d_{\alpha N(i+1)}$, $d_{\beta N(i+1)}$ and $d_{NN(i+1)}$ NOEs.

The mixing time of 150 ms was used after a NOE buildup analysis (not shown). At this mixing time there is no spin diffusion.

All peptides showed very poor NOESY spectra at 20°C (Figs. 1b, 2b and 3b). There could be two causes for that: one is because of the tumbling rate of the peptide that generates NOEs with near zero intensity; the other is because the peptide could be very flexible in solution not showing sequential NOEs. We observed that for all three peptides at 20°C the intra-residue NOEs could be observed at mixing times higher that 300 ms. When we dropped the temperature to 5°C we were able to detect several NOE cross-peaks, both short-range or long-range. The low temperature could be stabilizing some structure and/or decreasing the tumbling rate, making non-zero NOEs.

All three peptides displayed dispersed peaks with sharp lines, compatible with the small molecular mass (~1.3 kDa) and high water solubility. Table 2 summarizes the observed structural features of the peptides in solution. The total number of assigned NOEs varied among 103 to 127. Most of the NOEs were intra-residue and sequential. Peptide R13 did not show any long-range NOE (more than four residues apart) and only two medium-range NOEs, suggesting that this peptide behaves as a random coil in solution, not showing any structural tendency.

Peptide H13, on the other hand, showed 15 medium- and long-range NOEs. The important constraints to define a structural tendency are listed in Table 2. Peptide A13 also showed nine medium- and long-range NOEs. A well-defined structural tendency could also be noted for both A13 and H13 (Table 2).

3.2. Structure calculation

The structure calculation was performed using distance restraints obtained from NOE spectra at 5°C (Table 2). Structural statistics of the 20 lowest energies are also shown in Table 2. The program Procheck_NMR [27] was used for validating the geometries of the structures. Ramachandran plots [28] show that the majority of the dihedral angles are in the allowed region (>91% in favored regions).

RMSD values are also compatible with flexible topologies. However, there are noticeable differences between R13, H13 and A13. For R13 there is no convergence after structural calculation (Table 2). This is not surprising since we expected peptide R13 to be in random coil conformation.

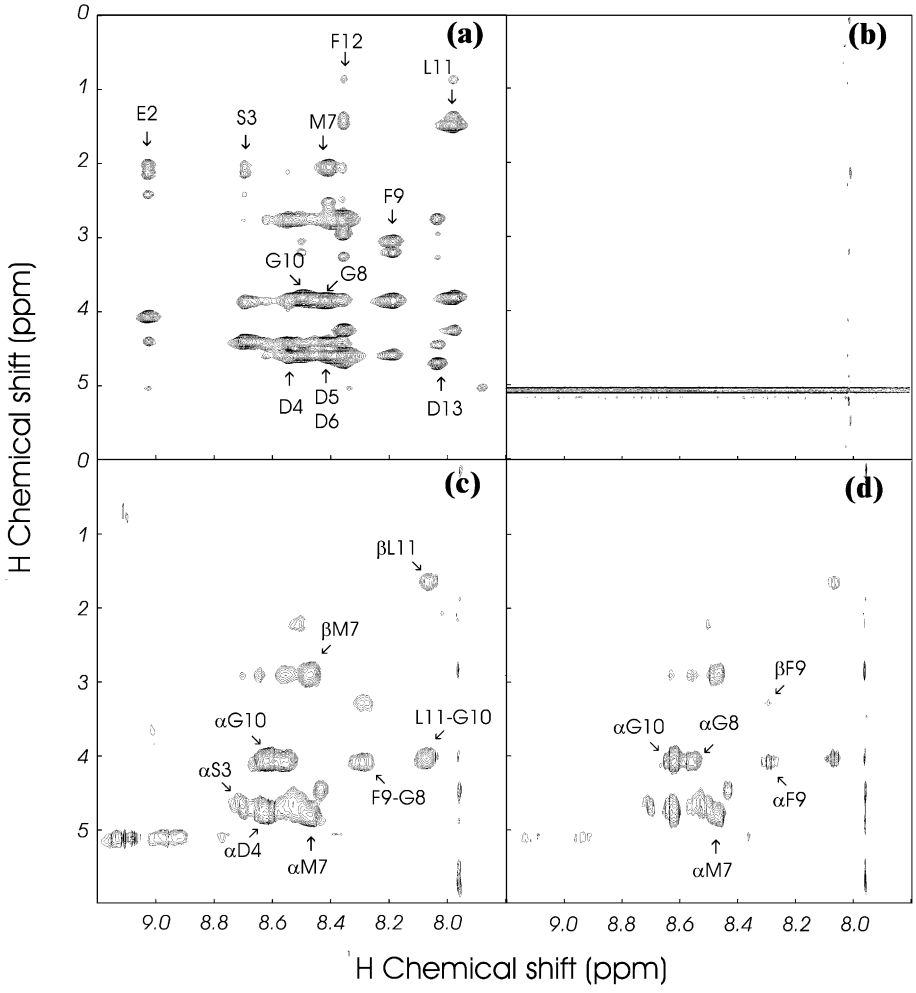

Fig. 2. Amide region of ^{1}H NMR spectra of H13 in phosphate buffer. a: NOESY spectrum at 5°C of 2 mM H13, 80 scans. b: NOESY spectrum at 20°C of 2 mM H13, 80 scans. c: Transfer NOESY spectrum of the mixture of 1 mM H13 and 50 μM pAb at 20°C, 384 scans. d: Transfer NOESY spectrum of the mixture of 1 mM H13 and 10 μM mAb at 20°C, 384 scans.

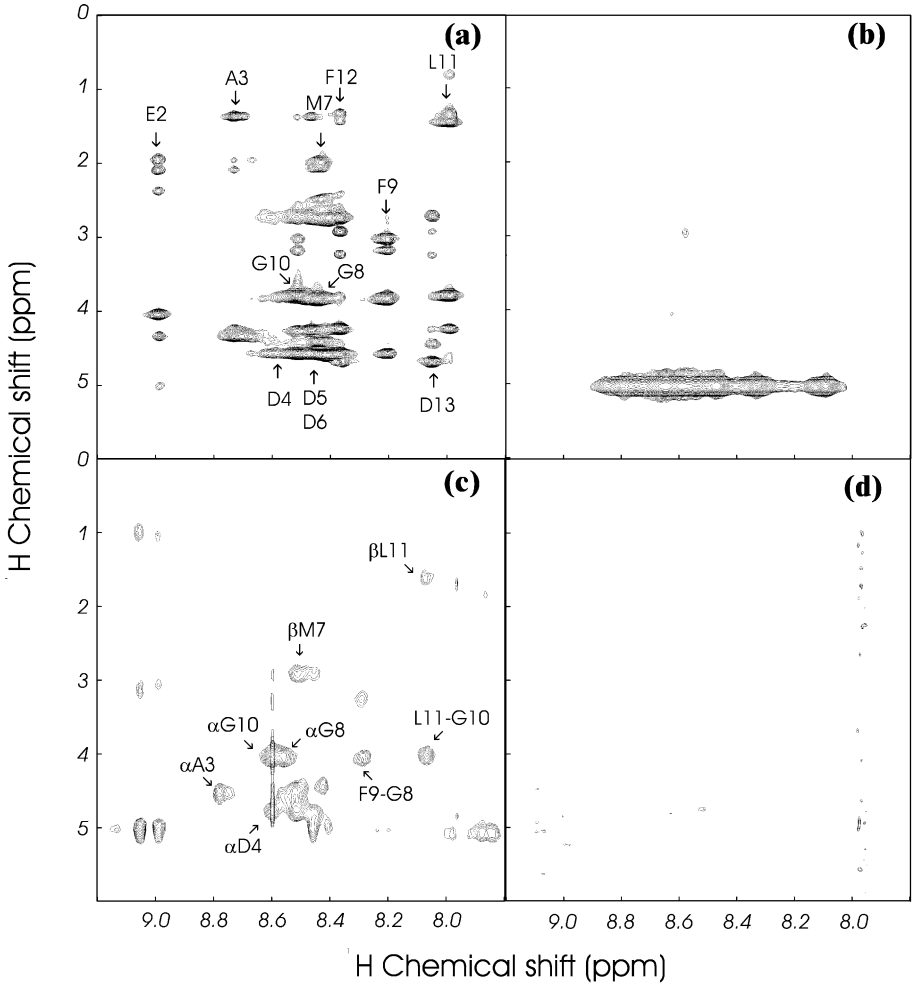

Fig. 3. Amide region of ^{1}H NMR spectra of A13 in phosphate buffer. a: NOESY spectrum at 5°C of 2 mM A13, 80 scans. b: NOESY spectrum at 20°C of 2 mM A13, 80 scans. c: Transfer NOESY spectrum of the mixture of 1 mM A13 and 50 μM pAb at 20°C, 384 scans. d: Transfer NOESY spectrum of the mixture of 1 mM A13 and 10 μM mAb at 20°C, 384 scans.

For peptides H13 and A13 we were able to calculate well-defined structures. Fig. 4 shows the 20 lowest energy structures obtained for the peptides H13 and A13. In both H13 and A13 structures, we observed a hydrophobic core formed by Met7, Phe9, Leu11 and Phe12. This hydrophobic core is not stable in R13 probably due to the presence of the negative residue Glu3 that increases electrostatic repulsion and leads the peptides to a random coil conformation. Ala3/Ser3 (A13 and H13 respectively) are in close proximity to the hydrophobic core, contributing to its stabilization. For peptide A13, Ala3 is interacting with Phe12 by hydrophobic interaction, while for peptide H13, Ser3 is interacting with the side chain of Met7, possibly by hydrogen bond.

The presence of the hydrophobic core leads to a bend of the

Table 2
Summary of structural statistics for free peptides in phosphate buffer at 5°C

	R13	H13	A13
Total number of distance constraints	109	127	103
Number of intra-residue constraints	82	74	67
Number of sequential and medium-range constraints ($\leq i,i+3$)	27	51	33
Number of long-range constraints ($\geq i,i+4$)	0	2 S3(H_N)-M7(Hβ) D5(H_N)-L11(H_N)	3 F9(Hβ)-D13-(Hβ) FM7(Hβ)-F12(Hδ) A3(Hβ)-F12(Hδ)
Overall energy (kcal/mol)	–	80.8 ± 18.3	92.6 ± 10.1
Pairwise RMSD (Å) of the residues 2–12[a]			
Backbone	1.38	0.63	0.49
Heavy atoms	1.98	0.94	0.76
% of the residues in favored region of the Ramachandran plot[b]	91.1	99.4	100

[a]RMSD values from MOLMOL [24].
[b]Data from PROCHECK [29].

peptides H13 and A13, where Asp4, Asp5 and Asp6 are the hinge region. The 20 models of lowest energy present a good overlap, especially in the bend region.

3.3. Transfer NOESY

Transferred NOE experiments were performed using IgG purified from cChHD patients' sera and a monoclonal IgG obtained against *T. cruzi* ribosomal P protein. We investigated conformational differences between the three peptides in free and bound states at 20°C. We used the ratio 1:20 for the pAb and 1:100 for the mAb.

The addition of the pAb (1:20) at pH 7.0 broadened the resonances of the peptides. This is due to the binding process. We then decreased the pH to 6 and 5. The lines sharpened progressively. We chose to work at pH 6.0 because of the sharp lines and appearance of several cross-peaks in the NOESY in the presence of the pAb (Figs. 1c, 2c and 3c) spectra, when compared to the NOESY spectra of the peptides free in solution at the same conditions (Figs. 1b, 2b and 3b).

At pH 6.0 and 20°C the peptide/antibody complex achieved a fast exchange regime. The appearance of NOEs is good evidence of binding, because of the decrease in the tumbling rate, making the peptides behave as a larger protein.

None of the medium- and/or long-range NOEs that define the structure calculated in aqueous solution at 5°C (Fig. 4) could be observed in the transfer NOESY experiments (Figs. 1c, 2c and 3c). The absence of these NOEs, however, is not due to the lower peptide concentration in the experiments in the presence of antibody, since the number of scans was almost five times higher in the presence of antibody while the concentration is halved. This suggests that the structure (bend) obtained for the peptides A13 and H13 was disrupted upon binding with the antibody. The conformation in the presence of antibody could not be determined because of the lack of long-range NOEs. This may imply that under these conditions the peptides assume an extended conformation.

A defined extended conformation in the presence of antibody is corroborated by the presence of sharp lines and some intra-residue NOEs, mostly connecting adjacent residues (αN, *i*,*i*+1). The presence of intra-residue NOEs for most of the amino acid sequence, from 3 to 12, is also noteworthy.

The interaction of the peptides with the mAb was limited by the amount of antibody. However, the number of NOEs observed in the transfer NOESY spectra of peptides R13, H13 and A13 (Figs. 1d, 2d and 3d) correlates with the binding ability. Note that peptide A13 does not bind to the mAb, or binds at low affinity. The number of transfer NOEs for peptide R13 is higher than for peptide H13.

A similar observation can be made on the interaction with the pAbs. The number of observed NOEs in the transfer NOESY spectra is bigger for peptide R13 (Fig. 1c) than H13 (Fig. 2c) and A13 (Fig. 3c), in the same order as observed for the

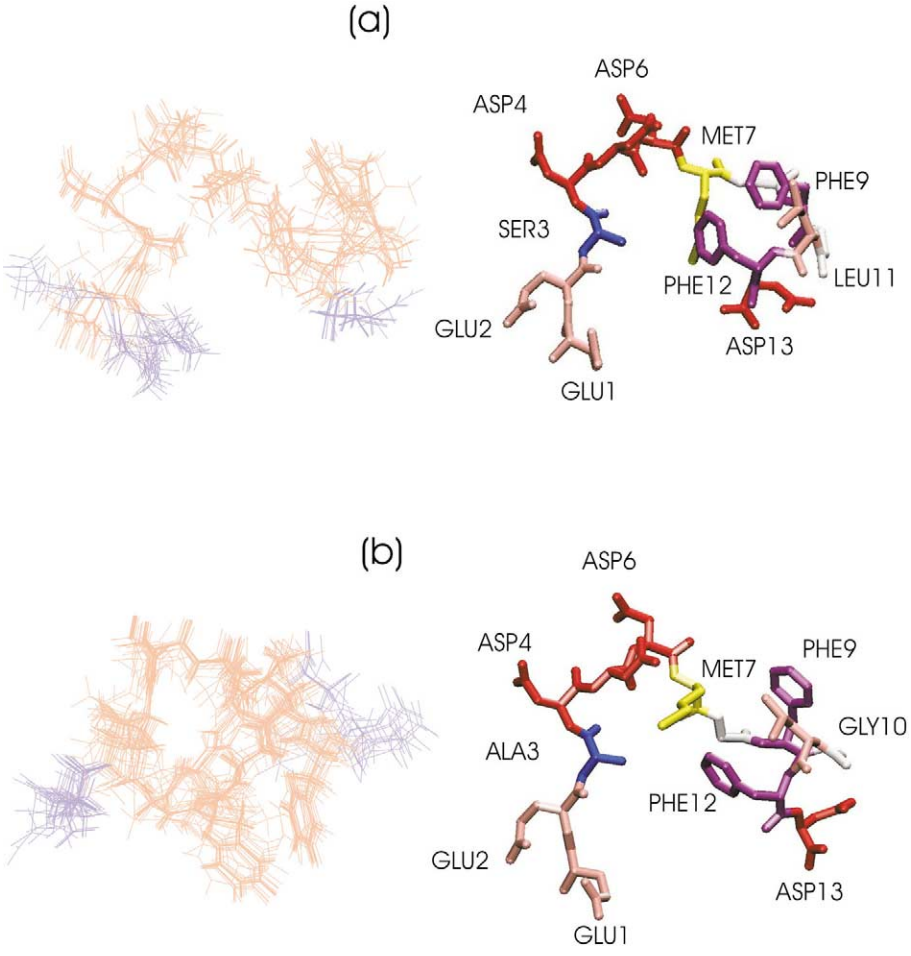

Fig. 4. Twenty lowest energy structures calculated for the peptides in phosphate buffer at pH 5.5 and 5°C (left) and lowest energy structure (right). a: H13. b: A13.

interaction with the mAb: R13 > H13 > A13. This order is inverse when compared with the presence of structure of the free peptides in solution. A13 shows better resolution in the backbone than H13, while R13 does not show any structural tendency. The rationale is that the presence of structure in the free state leads to a decrease in the binding affinity.

The fact that peptide A13 does not interact with the mAb is in accordance with the work of Mahler et al. [15]. In this work, the authors tested the importance of each amino acid in the mAb recognition by alanine mutation scanning. They concluded that the amino acids essential for recognition were Glu3, Asp5, Asp6, Gly8 and Phe9.

4. Discussion

Peptides that correspond to epitope regions of proteins are widely used as synthetic antigens, vaccines or diagnostic reagents. They have been extensively studied to understand their antigenicity and immunogenicity in an effort to develop effective new chemotherapeutic drugs and vaccines. Although simple models, they are not completely understood. Epitopes are usually classified as linear or conformational depending on requirements for antibody recognition.

In the present work, we describe the solution structure of three peptides: R13, H13 and A13. They represent the epitope regions of ribosomal P proteins that seem to be responsible for autoimmune responses observed in cChHD patients. There is only one amino acid difference between them. This difference could be considered innocuous for a given linear epitope, since the major feature of the epitope is maintained, the negative charge. But several results show differences in antibody recognition between them [14,15].

Using this simple model we decided to investigate what could be structurally responsible for the observed differences. The peptides were studied in the free and antibody-bound state. Peptides are known to be flexible in solution due to the lack of long-range interaction. NMR studies are then suitable to monitor the behavior in solution.

We investigated the structure at 5°C and the obtained NOESY spectra permitted structural calculations. Peptide R13 is in random coil conformation. Peptides H13 and A13 showed well-defined structures in solution. Change of only one amino (residue 3) acid residue is enough to modify the peptide structure in solution. Both peptides formed a bend stabilized by interactions in which residue 3 participates (Ser3 and Ala3).

The addition of antibody (50 μM pAb and 10 μM mAb) in usual conditions (pH 7.0) creates line broadening in the peptide spectra, indicating an effective binding with antibodies. This line broadening reflects the slow exchange between the bound and free peptide states. A decrease in pH makes the line narrow, indicating a fast exchange between the bound and free peptide states. This condition is appropriate to transfer NOE experiments. Then, the transfer NOESY experiments were carried out at 20°C and the results were good quality spectra with several correlation peaks. The observed NOEs were exclusively from the bound state since the spectra of the peptides free in solution do not show NOEs at this temperature (20°C).

The spectra present some correlation peaks, including inter-residuals. This indicates that the presence of antibody reduces the peptide flexibility at 20°C probably inducing a more defined conformation. The absence of long-range correlation indicates an extended conformation for these peptides in the bound state.

Various antibody–epitope complexes are formed with peptides in extended conformation, for example, the region between residues 101–108 of influenza hemagglutinin complexed with its antibody [29] and the peptide corresponding to residues 308–333 of the HIV Gp120 with IgG Fab [30].

These observations suggest that for the pAb recognition specific folding is not necessary.

Due to the fact that the peptide–antibody does not require a specific conformation for the peptide, the possibility of the existence of cross-reaction is increased. Then, considering that for an autoimmune process a cross-reaction is necessary, our findings favor this hypothesis.

Our data indicate that the binding of R13 is more efficient because it is a random coil in solution whereas R13 and A13 do not bind so efficiently because they show a structural tendency free in solution, with a conformation different from the bound state. There is an increasing notion in the literature that the pre-existence of the bound conformation in the free state is fundamental for binding [31]. In the present work we have strong evidence that conformational states are important, although we could not rule out the direct influence of the amino acid change in the peptides in the affinity to the antibody.

5. Notes

The coordinates were deposited in the Protein Data Bank with the following codes: 1S4H and 1S4J. The chemical shift assignment tables were deposited in the Biomagnetic Resonance Data Bank.

Acknowledgements: This work was supported by grants from the Conselho Nacional de Desenvolvimento Científico e Tecnológico (CNPq) and NIH Grant 1R01 HL 073732-01.

References

[1] Chagas, C. (1909) Mem. Inst. Oswaldo Cruz 1, 159–218.
[2] Brener, Z. and Andrade, Z. (Organizers) (1979) *Trypanosoma cruzi* e doença de Chagas, Guanabara Koogan, Rio de Janeiro.
[3] Brener, Z. (1992) Immune response and immunopathology in *Trypanosoma cruzi* infection in Chagas' disease (American trypanosomiasis): Its impact on transfusion and clinical medicine (Wendel, S., Brener, Z., Camargo, M.E. and Rossi, A., Eds.), São Paulo.
[4] Borda, E., Pascual, J., Cossio, P., Delavega, M., Arana, R. and Sterin-Borda, L. (1984) Clin. Exp. Immunol. 57, 679–686.
[5] Leon, J.S. and Engman, D.M. (2001) Int. J. Parasitol. 31, 555–561.
[6] Cunha-Neto, E. (1995) Rev. Soc. Cardiol. São Paulo 5, 217.
[7] Cunha-Neto, E., Duranti, M., Gruber, A., Zingales, B., de Messias, I., Stolf, N., Bellottti, G., Patarroyo, M.E., Pilleggi, F. and Kalil, J. (1995) Proc. Natl. Acad. Sci. USA 92, 3541–3545.
[8] Kaplan, D., Ferrari, I., Bergami, P.L., Mahler, E., Levitus, G., Chiale, P., Hoebeke, J., Van Regenmortel, M.H.V. and Levin, M.J. (1997) Proc. Natl. Acad. Sci. USA 94, 10301–10306.
[9] Levin, M.J., Mesri, E., Benarous, R., Levitus, G., Schijman, A., Levy-Yeyati, P., Chiale, P., Ruiz, A.M., Kshn, A., Rosenbaum, M., Torres, H.N. and Segura, E.L. (1989) Am. J. Trop. Med. Hyg. 41, 530–539.
[10] Levin, M.J., Levitus, G., Kerner, N., Lafon, S., Schijman, A., Levy-Yeyati, P., Finkieltstein, C., Chiale, P., Schejtman, D. and Hontebeyrie-Joskowicz, M. (1990) Mem. Inst. Oswaldo Cruz 85, 539–543.
[11] Mesri, E.A., Levitus, G., Hontebeyrie-Joskowicz, M., Dighiero,

G., Van Regenmortel, M.H.V. and Levin, M.J. (1990) J. Clin. Microbiol. 28, 1219–1224.
[12] Levitus, G.M., Hontebeyrie-Joskowicz, M., Van Regenmortel, M.H.V. and Levin, M.J. (1991) Clin. Exp. Immunol. 85, 413–417.
[13] Ferrari, I., Levin, M.J., Wallukat, G., Elies, R., Lebesgue, D., Chiale, P., Elizari, M., Rosenbaum, M. and Hoebeke, J. (1995) J. Exp. Med. 182, 59–65.
[14] Masuda, M.O., Levin, M.J., Oliveira, S.F., dos Santos Costa, P.C., Bergami, P.L., Almeida, N.A.S., Pedrosa, R.C., Ferrari, I., Hoebeke, J. and Campos de Carvalho, A.C. (1998) FASEB J. 12, 1551–1558.
[15] Mahler, E., Sepulveda, P., Jeannequin, O., Liegeard, P., Gounon, P., Wallukat, G., Eftkhari, P., Levin, M.J., Hoebeke, J. and Hontebeyrie, M. (2001) Eur. J. Immunol. 31, 2210–2216.
[16] Piotto, M., Saudek, V. and Sklenar, V. (1992) J. Biomol. NMR 2, 661–665.
[17] Bax, A. and Davis, D.G. (1995) J. Magn. Reson. 65, 355–360.
[18] Sklenar, V., Piotto, M., Leppek, R. and Sandek, V. (1993) J. Magn. Reson. Ser. A 102, 241–245.
[19] Mayo, K.H. (1997) Methods Enzymol. 289, 646–672.
[20] Delaglio, F., Grzesiek, S., Zhu, G., Vuister, G.W., Pfeifer, J. and Bax, A. (1995) J. Biomol. NMR 6, 277–293.
[21] Johnson, B.A. and Blevins, R.A. (1994) J. Biomol. NMR 4, 603–614.
[22] Hyberts, S.G., Goldberg, M.S., Havel, T.F. and Wagner, G. (1992) Protein Sci. 1, 736–751.
[23] Brünger, A.T., Adams, P.D., Clore, G.M., DeLano, W.L., Gros, P., Grosse-Kunstleve, R.W., Jiang, J.S., Kuszewski, J., Nilges, M., Pannu, N.S., Read, R.J., Rice, L.M., Simonson, T. and Warren, G.L. (1998) Acta Crystallogr. D 54, 905–921.
[24] Stein, E.G., Rice, L.M. and Brüger, A.T. (1997) J. Magn. Reson. 124, 154–164.
[25] Koradi, R., Billeter, M. and Wüthrich, K. (1996) J. Mol. Graphics 14, 51–55.
[26] Wüthrich, K. (1986) NMR of Proteins and Nucleic Acids, Wiley-Interscience, New York.
[27] Ramanchandran, G.N. and Sasisekharan, V. (1968) Adv. Protein Chem. 23, 283–437.
[28] Laskowski, R.A., Rullmann, J.A.C., MacArthur, M.W., Kaptein, R. and Thornton, J.M. (1998) J. Biomol. NMR 8, 477–486.
[29] Churchill, M.E.A., Stura, E.A., Pinilla, C., Appel, J.R., Houghten, R.A., Kono, D.H., Balderas, R.S., Fieser, G.G., Schulze-Gahmen, U. and Wilson, I.A. (1994) J. Mol. Biol. 241, 534–556.
[30] Stanfield, R.L., Cabezas, E., Satterthwait, A.C., Stura, E.A., Profy, A.T. and Wilson, I.A. (1999) Structure 7, 131–142.
[31] Volkman, B.F., Lipson, D., Wemmer, D.E. and Kern, D. (2001) Science 291, 2429–2433.